Longitudinal Flow Along Circular Cylinders and Thick Plates, Including Blunt Leading-Edge Separation

A. Halim*
Air Force Institute of Technology, Wright-Patterson Air Force Base, Ohio
and
U. Ghia†
University of Cincinnati, Cincinnati, Ohio

The axisymmetric flow over a class of bodies of revolution with an external shoulder, as well as the corresponding two-dimensional flow, are studied using the incompressible Navier-Stokes equations formulated in terms of surface-oriented conformal coordinates and similarity-type vorticity and stream-function variables. A factored ADI scheme is used to obtain numerical solutions of the coupled governing equations for various values of the problem parameters. For the case of sharp-shouldered thick plates, the effect of the Reynolds number on the length of the recirculating region is presented and good agreement is obtained with the corresponding experimental data. Results are then obtained for axisymmetric flow past longitudinal cylinders; these compare well with the boundary-layer solutions at some stations far downstream.

Introduction

WILLIAMS[1] has reviewed the status of the research on incompressible laminar flow separation. While a considerable body of literature exists on the analysis of two-dimensional external flows in infinite domains using the Navier-Stokes equations, the same is not true for axisymmetric flows. The work most relevant to the present research is the analysis by Davis and Werle[2] of axisymmetric flow past a paraboloid of revolution at zero angle of incidence. The only experimental work related to the present study is that of Lane and Loehrke,[3] who measured the length of the recirculating-flow region for two-dimensional configurations with a sharp shoulder.

The present study adds to the available research on the subject of laminar incompressible flow separation and represents an extension of the two-dimensional flow-separation analysis of Ghia and Davis.[4] Several aspects of the research are of a fundamental nature, and should be useful in general external as well as internal flow applications.

Analysis

The flow problem is formulated using the complete Navier-Stokes equations in terms of similarity-type stream function and vorticity variables and conformal coordinates in the meridional plane, as shown in Fig. 1. The formulation is generalized by the use of an index j such that $j=1$ for axisymmetric flow and $j=0$ yields the two-dimensional case. The other parameters in the formulation are the flow Reynolds number Re and a geometrical parameter η_w related to the curvature of an external shoulder in the body surface. For some combinations of Re and η_w, the flow encounters separation downstream of the body shoulder. The cases with $\eta_w=0$, i.e., bodies with a sharp shoulder, encounter separation at fairly low Re. In fact, these configurations are of particular concern in the present study and correspond to the longitudinal flow along circular cylinders (or slabs for two-dimensional cases with $j=0$) with blunt leading faces.

The physical variable $z=r-ix$ and the conformal variable $\zeta=\xi+i\eta$ are related by the conformal transformation

$$z=\tfrac{1}{2}\left[\zeta(Re-\zeta^2)^{1/2}+Re\,\sin^{-1}(\zeta/\sqrt{Re})\right] \tag{1}$$

The corresponding scale factors are obtained as

$$h_1=h_2=h=\left|\frac{dz}{d\zeta}\right|=\left[(\xi^2+\eta^2-Re)^2+4Re\,\eta^2\right]^{1/4} \tag{2}$$

The scale factor h_3 along the third direction is given as

$$h_3=H=r^j \tag{3}$$

The Reynolds number Re appearing in Eqs. (1) and (2) is defined as

$$Re=(2/\pi)U_\infty d/\nu \tag{4}$$

with d taken to be the diameter of the circular cylinder for axisymmetric flow, or the thickness of the plate for two-dimensional cases.

The introduction of similarity variables facilitates the analytical extraction of some of the known variation of the flow from the physical dependent variables. The rate of spatial variation in terms of the similarity variables themselves is thereby considerably reduced. The following relations define these new variables:

$$\psi(\xi,\eta)=\xi^{j+1}f(\xi,\eta) \tag{5}$$

$$\Omega(\xi,\eta)=-\left[(\xi^{j+1}/Hh^2)\right]g(\xi,\eta) \tag{6}$$

However, when $j=1$, g increases with η_w. Also, $f\to\infty$ as $\eta=\infty$. Hence, the following new dependent variables are introduced for the vorticity and stream function:

$$G=g/(Re+\eta_w^2)^{j/2} \tag{7}$$

$$F=f-(\eta^{j+1}-\eta_w^{j+1})/(j+1) \tag{8}$$

so that F and G remain bounded and of order unity everywhere.

A bounded computational domain is achieved by the introduction of the new independent variables S and N, defined via appropriate transformations based on those used earlier by Davis and Werle[2] and Ghia and Davis,[4] and given as

Presented as Paper 82-0024 at the AIAA 20th Aerospace Sciences Meeting, Orlando, FL, Jan. 11-14, 1982; received Sept. 25, 1986.

*Associate Professor, Department of Aeronautical and Astronautical Engineering; formerly, Graduate Assistant, University of Cincinnati, OH. Senior Member AIAA.
†Professor. Associate Fellow AIAA.

follows:

$$N=(\eta-\eta_w)/(C+\eta-\eta_w) \tag{9}$$

and

$$S=1-a(A_t/\xi)\ell n(1+\xi/A_t)+e\tan^{-1}(\xi-\xi_c)+c \tag{10}$$

where $\xi_c=\sqrt{Re}$, the value of ξ at the shoulder, and a, A_t, e, c, and C are arbitrary constants evaluated from specified conditions for the transformation and the degree of the resolution required. The transformation given by Eq. (10) also provides some clustering of mesh points in the vicinity of the shoulder.

The *differential equations* governing the flow consist of the Navier-Stokes equations expressed in terms of the vorticity G and the stream function F using S and N as the independent variables. The *boundary conditions* consist of zero slip at the wall and the prevailing inviscid flow as $\eta\to\infty$. As $\xi\to\infty$, all derivatives with respect to ξ vanish, and the resulting self-similar form of the governing equations are ordinary differential equations whose solution provides the downstream boundary conditions for the present flow problem. On the symmetry line, F_ξ and G_ξ are zero, as are H and H_η. Rather than using these conditions directly, they are employed in the governing equations to obtain special forms of the equations which are then solved to determine the solution at this boundary. However, due to the presence of the $F_{\xi\xi}$ and $G_{\xi\xi}$ terms in these equations, the solution at this boundary must evolve iteratively along with the overall solution in the interior of the computational domain.

Algorithm for Numerical Solution

The numerical scheme that seems to be efficient for this problem is the factored alternating-direction implicit (FADI) scheme of Beam and Warming.[5] This scheme was extended by Hill et al.[6] to solve, simultaneously, the system of difference equations resulting from the two partial differential equations governing the vorticity and the stream function for the flow. The details of the application of FADI and the derivation of the factored form of the equations governing the present problem, as well as the means for optimizing the numerical solution procedures, are given by Ghia and Halim.[7] The implicit implementation of the surface-boundary condition is described in detail in Ref. 8. An incremental formulation is employed and all spatial derivatives in the governing equations are represented by second-order-accurate central-difference expressions, except for the streamwise convective term in the vorticity equation. This convective term in the incremental variable is represented by an upwind difference, which is first-order-accurate, while retaining a second-order-accurate central difference for this convective term in the variable itself. This lends the desired stability and convergence property to the evolving solution, while restoring second-order accuracy in the steady-state solution. For forward flow, the streamwise convective term is treated implicitly in the normal sweep, thus honoring the overall boundary-layer-like features of the flow.

Results and Discussion

Tests showed that, as Re increases, the use of upwind differencing for the streamwise convective term increased the allowable time step by an order of magnitude, with a corresponding increase in the convergence rate of the solution and no significant degradation in accuracy of the steady-state solution. In fact, the results shown in Fig. 2 for the thin flat-plate configuration confirm that, in the limit of vanishing step size, the skin-friction function at the leading edge approaches the same value, independent of the manner of representing the streamwise convective terms. This is an advantage of the formulation in which it is possible to use an upwind difference for the derivative of the unknown vorticity increment that vanishes as convergence is approached, while retaining a central difference for the vorticity derivative itself. However, this increased rate of convergence was apparent only for moderate to high Re configurations. For the case of the thin flat plate, $Re=0$ in the present formulation, and the manner of treating the convective terms had no influence on the convergence rate or the magnitude of the computational time step used.

Solutions were obtained for several axisymmetric configurations corresponding to various values of the parameters Re and η_w. The most interesting among these are the cases with $\eta_w=0$, i.e., cylinders in axial flow. Boundary-layer solutions were determined by Cebeci[9] and Stewartson[10] for these configurations and serve as a partial check for the present solutions. The results obtained from the present computations are seen (Table 1) to be in good agreement with those of Cebeci[9] and Stewartson[10] at two stations far downstream. This is as should be expected, because the

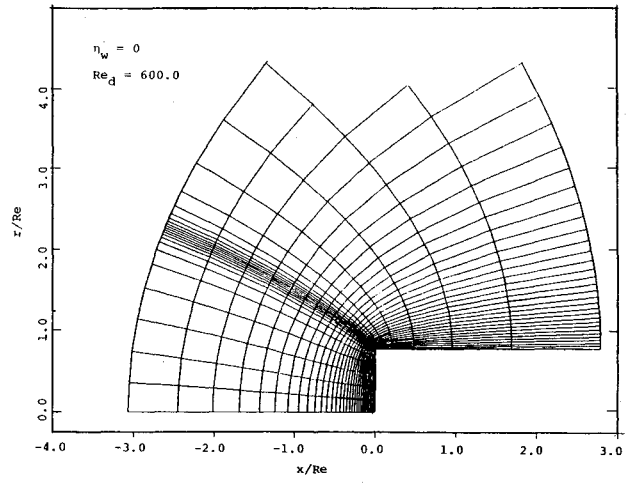

Fig. 1 Coordinate distribution with resolution at sharp shoulder.

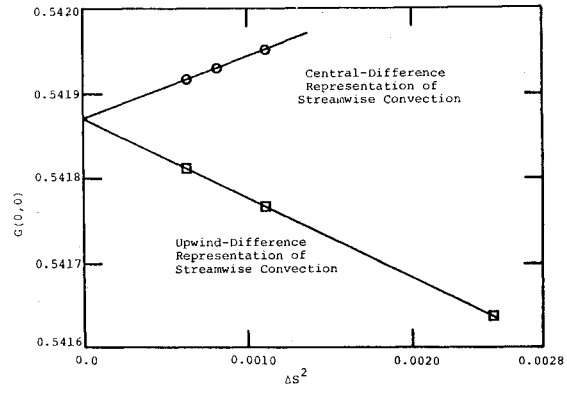

Fig. 2 Analysis of accuracy of vorticity-function at leading edge of flat plate.

Table 1 Comparison of the vorticity function at downstream positions along the cylinder

Re	ξ	Present (Navier-Stokes)	Cebeci[9] (Boundary layer)	Stewartson[10] (Series solution)
200	1108.009	0.03346	0.030407	0.03026
300	3347.318	0.02303	0.020932	0.02067
	1366.011	0.02895	0.0260534	0.025932
400	3879.399	0.0206	0.0181	0.0185
	1583.431	0.02617	0.0233	0.0233
600	4771.66	0.0177		0.01592
	1947.958	0.023	0.0203	0.0196

ellipticity in the present formulation of the Navier-Stokes equations diminishes with distance downstream, and their solution asymptotically approaches the solution of the boundary-layer equations far downstream. Figure 3 shows the surface distribution of the vorticity function $G(\xi,\eta_w)$ for the cases presented in Table 1. Immediately downstream of the shoulder, the vorticity function decreases sharply due to the large adverse pressure gradient at the shoulder, causing the flow to separate. Downstream thereof, the pressure gradient starts to approach zero and the flow reattaches, approaching the boundary-layer solution downstream and finally attaining the self-similar solution at downstream infinity. Also, as Re increases, the separation point moves upstream and the reattachment point moves downstream, leading to an increase in the extent as well as the intensity of the separated flow. At large distances downstream, the value of G decreases as Re increases. In the limit as $Re\to\infty$, for axisymmetric flow, the limit of $G\sqrt{Re}$ would be the two-dimensional Blasius value (0.47), because the transverse curvature effects become negligible as $Re\to\infty$.

Figure 4 shows a comparison of the surface distribution of the vorticity function for axisymmetric and two-dimensional configurations. As should be expected, the results predict that axisymmetric separation is, in general, less severe than two-dimensional separation.

Figures 5-8 show the streamline contours for the same flow configurations for which the vorticity function G was presented in Fig. 3. The nondimensional stream function $\bar{\psi}$ depicted in Figs. 5-8 is related to the nondimensional ψ used in the derivation of the governing equations as $\bar{\psi}=\psi/Re^{j+1}$. The values of the stream function along the contours are the same for all the cases presented in Figs. 5-10 to enable direct comparison of the results in these figures and deduce some qualitative features of the behavior of the flow as Re increases. At $Re=200$, the flow barely separates; although this is not visible from Fig. 5, it is distinctly seen by the negative value of the surface-vorticity function encountered by the corresponding G distribution (Fig. 3). At $Re=300$, the separation bubble increases in strength as well as size (Fig. 6). The length of the separation bubble continues to increase as Re is increased from 400 to 600. At $Re=600$, the recirculating bubble length is approximately 1.5 times the cylinder diameter. Incidentally, this value is not very different from the value of 1.6 reported by Ota[11] for the recirculating bubble length for turbulent flow over a longitudinal cylinder. In the turbulent-flow range of Re, the recirculation length was observed by Ota[11] to be independent of Re. It is possible that this may be so for the laminar case also for large Re.

In order to further compare or contrast the axisymmetric flow pattern from the corresponding two-dimensional flow configurations, Fig. 9 shows the streamline contours for the two-dimensional configuration at $Re=300$. It is seen that the length of the recirculating region for the two-dimensional case is approximately 10 times that for the axisymmetric case (Fig. 6). As shown later in Fig. 11, experimental measurements reveal that the recirculating length attains a maximum

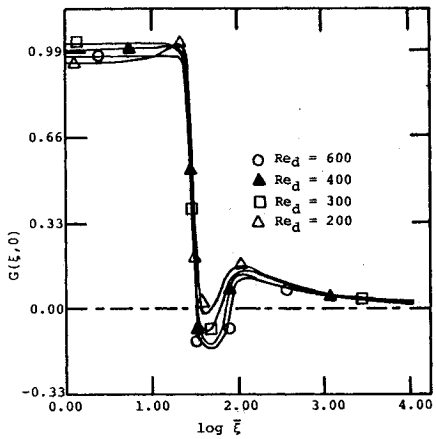

Fig. 3 Effect of Re on vorticity-function distribution on surface of longitudinal cylinder.

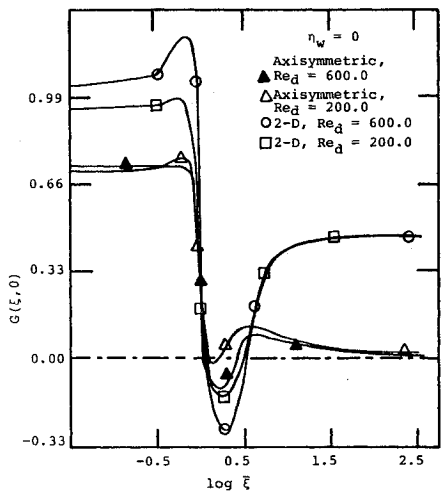

Fig. 4 Comparison of vorticity-function distribution on surface of two-dimensional and axisymmetric bodies with sharp shoulder.

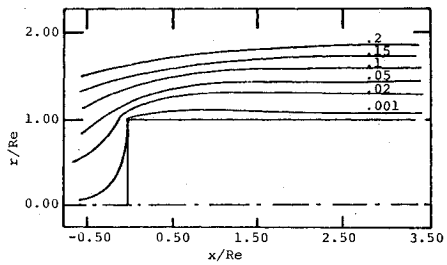

Fig. 5 Streamline configuration for flow past longitudinal cylinder, $Re=200$.

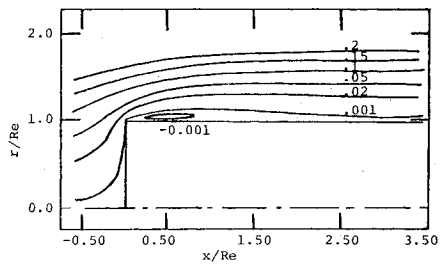

Fig. 6 Streamline configuration for flow past longitudinal cylinder, $Re=300$.

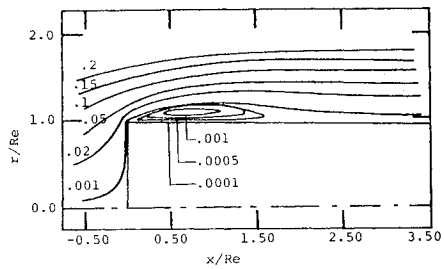

Fig. 7 Streamline configuration for flow past longitudinal cylinder, $Re=400$.

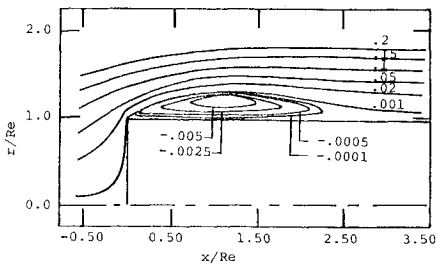

Fig. 8 Streamline configuration for flow past longitudinal cylinder, $Re = 600$.

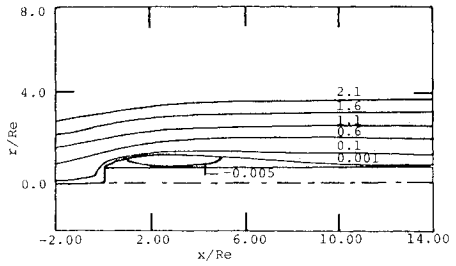

Fig. 9 Streamline configuration for two-dimensional flow, $Re = 300$.

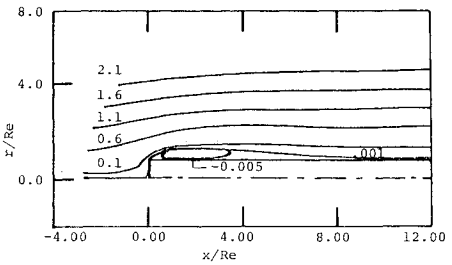

Fig. 10 Streamline configuration for two-dimensional flow, $Re = 600$.

value for the two-dimensional case at $Re = 300$. Figure 10 shows the streamline contours for the two-dimensional flow configuration at $Re = 600$. Comparison of this result with the corresponding result for the axisymmetric flow pattern (Fig. 8) shows that the ratio of the length of the recirculating region for the two-dimensional case to that for the axisymmetric case is approximately 2.6. It is remarkable that this is nearly the same value as obtained from the experimental measurements of Ota[11] and Ota and Itasaka[12] for two-dimensional and axisymmetric flows in the turbulent-flow range of *Re*. It is possible that this represents the asymptotic value of this ratio for large *Re* for the flows considered, irrespective of whether the flow is laminar or turbulent.

The only experimental data available for possible comparison with the present solutions are those provided by Lane and Loehrke[3] for the length of the recirculating flow region for two-dimensional configurations. These are shown in Fig. 11. As the mean curve in the figure indicates, the recirculating length approaches a constant value of about 4.5 plate thicknesses beyond $Re \simeq 600$. Also included is the two-dimensional experimental result of Ota and Itasaka,[12] who reported that even in the turbulent flow regime the recirculation length remains approximately 4–5 times the plate thickness. The measurements of Ota[11] for the corresponding axisymmetric turbulent flow indicate that the recirculation length is approximately 1.6 times the cylinder diameter, i.e., nearly one-third for the two-dimensional case. The results of the present computations are shown by solid symbols in Fig. 11. For two-dimensional calculations, the results are in good agreement with the data of Lane and Loehrke.[3] The computational predictions for the corresponding axisymmetric configurations show a considerable reduction in the recirculation length, in conformity with the measurements of Ota and his coworkers (Refs. 12 and 11) for the two-dimensional and axisymmetric cases in the turbulent-flow regime. Also, the curve for the axisymmetric case is, in general, shifted toward the right, since the minimum value of *Re* at which separation first occurs is higher for the axisymmetric case than for the two-dimensional cases.

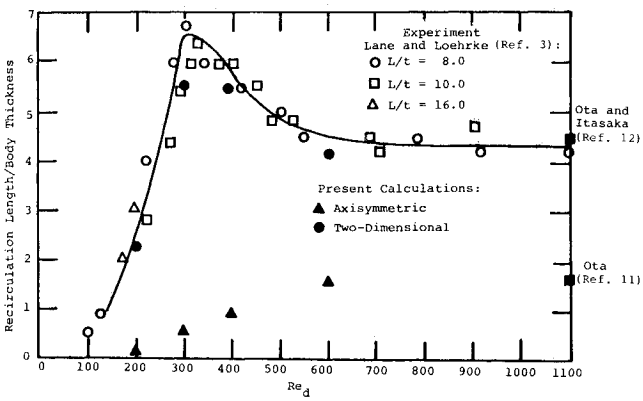

Fig. 11 Comparison of measured and computed recirculation lengths for blunt plates and longitudinal cylinders.

Acknowledgments

This research was funded in part by AFOSR Grant 80-0160, with Dr. James D. Wilson as Technical Monitor. The research is based on much that was learnt from Professor R. T. Davis, whose sudden passing away in January 1986 leaves an indescribable void and to whose memory this paper is dedicated.

References

[1]Williams, J., "Incompressible Boundary-Layer Separation," *Annual Reviews of Fluid Mechanics*, Vol. 9, 1977, pp. 113–144.

[2]Davis, R. T. and Werle, M. J., "Laminar Incompressible Flow Past a Paraboloid of Revolution," *AIAA Journal*, Vol. 10, Sept. 1972, pp. 1224–1230.

[3]Lane, J. C. and Loehrke, R. I., "Leading Edge Separation from a Blunt Plate at Low Reynolds Number," *Momentum and Heat Transfer Processes in Recirculating Flows*, ASME Publication HTD, Vol. 13, 1980, pp. 45–48.

[4]Ghia, U. and Davis, R. T., "Navier-Stokes Solutions for Flow Past a Class of Two-Dimensional Semi-Infinite Bodies," *AIAA Journal*, Vol. 12, Dec. 1974, pp. 1659–1665.

[5]Beam, R. M. and Warming, R. F., "An Implicit Factored Scheme for the Compressible Navier-Stokes Equations," AIAA Paper 77-645, 1977.

[6]Hill, J., Davis, R. T., and Slater, G., "Development of a Factored ADI Scheme for Solving the Navier-Stokes Equations in Streamfunction-Vorticity Variables," Aerospace Engineering Rept. AFL 79-12-49, Univ. of Cincinnati, Cincinnati, OH, 1979.

[7]Ghia, U. and Halim, A., "Navier-Stokes Solutions for Longitudinal Flow Along Circular Cylinder, Including Blunt Leading-Edge Separation," AIAA Paper 82-0024, Jan. 1982.

[8]Halim, A., Ghia, U., and Ghia, K. N., "Navier-Stokes Solutions for Incompressible Separated Flow Past a Glass of Two-Dimensional and Axisymmetric Semi-Infinite Bodies," Aerospace Engineering Rept. AFL 81-9-59, Univ. of Cincinnati, Cincinnati, OH, 1981.

[9]Cebeci, T., "Laminar and Turbulent Incompressible Boundary Layers on Slender Bodies of Revolution in Axial Flow," *Journal of Basic Engineering*, Vol. 92, 1970, pp. 545–554.

[10]Stewartson, K., "The Asymptotic Boundary Layer on a Circular Cylinder in Axial Incompressible Flow," *Quarterly Journal of Applied Mathematics*, Vol. 13, 1955, pp. 113–122.

[11]Ota, T., "An Axisymmetric Separated and Reattached Flow on a Longitudinal Blunt Circular Cylinder," *Journal of Applied Mechanics*, Vol. 42, No. 2, June 1975, pp. 311–315.

[12]Ota, T. and Itasaka, M., "A Separated and Reattached Flow on a Blunt Plate," *Journal of Fluids Engineering*, Vol. 98, 1976, pp. 79–86.